

See discussions, stats, and author profiles for this publication at: <https://www.researchgate.net/publication/231654984>

# Midinfrared Index Sensing of pL-Scale Analytes Based on Surface Phonon Polaritons in Silicon Carbide†

ARTICLE *in* THE JOURNAL OF PHYSICAL CHEMISTRY C · MARCH 2010

Impact Factor: 4.77 · DOI: 10.1021/jp9114139

CITATIONS

12

READS

13

6 AUTHORS, INCLUDING:



**Burton Neuner III**

Navy's Space and Naval Warfare Systems C...

27 PUBLICATIONS 286 CITATIONS

SEE PROFILE



**Dmitriy Korobkin**

University of Texas at Austin

44 PUBLICATIONS 707 CITATIONS

SEE PROFILE



**Davy Carole**

Claude Bernard University Lyon 1

44 PUBLICATIONS 137 CITATIONS

SEE PROFILE



**Gennady Shvets**

University of Texas at Austin

377 PUBLICATIONS 6,452 CITATIONS

SEE PROFILE

# Midinfrared Index Sensing of pL-Scale Analytes Based on Surface Phonon Polaritons in Silicon Carbide<sup>†</sup>

Burton Neuner III,<sup>‡</sup> Dmitriy Korobkin,<sup>‡</sup> Chris Fietz,<sup>‡</sup> Davy Carole,<sup>§</sup> Gabriel Ferro,<sup>§</sup> and Gennady Shvets<sup>\*,‡</sup>

Department of Physics, University of Texas at Austin, Austin, Texas 78712, and Laboratoire des Multimateriaux et Interfaces, Université Claude Bernard Lyon 1, 69622 Villeurbanne, France

Received: December 1, 2009; Revised Manuscript Received: February 20, 2010

We present the first demonstration of pL-scale analyte index sensing based on surface phonon polaritons in the midinfrared, which are excited at the silicon carbide/analyte interface in the Otto configuration. Attenuated total reflectance measurements reveal analyte index specificity through a double-scan of wavelength and incidence angle for analyte volumes as small as 100 pL. Midinfrared sensing tuned to surface phonon polariton resonance paves the way for index sensing of analytes beyond current volume–resolution limits.

Among the most desirable features of any refractive index sensing technique are (i) analyte specificity and (ii) small-volume sensitivity. The midinfrared (mid-IR) spectrum has long been employed in diverse sensing applications that include chemical spectroscopy, detection of atmospheric pollutants, and medical diagnostics because of its analyte specificity. Indeed, molecules exhibit unique spectroscopic fingerprints in the mid-IR that are manifested as larger index ( $n$ ) differences between materials in the mid-IR than in the visible. An example is shown in Figure 1, where the index difference between mineral oil and silicone oil is both larger than in the visible and wavelength-dependent. Recently, there has been growing interest in using resonant phenomena to improve upon mid-IR sensing, including enhanced biosensing that exploits Ni-mesh extraordinary infrared transmission<sup>1</sup> and gas index sensing based on surface wave excitation in prism-coupled Ti/Au layers<sup>2</sup> and silicon carbide gratings.<sup>3</sup> Resonant techniques are often needed for sensing because, e.g., weak vibrational modes contain detailed molecular information but are difficult to resolve without the aid of electric field enhancement.<sup>1</sup>

The requirement of small-volume sensitivity explains the widespread use of surface plasmon polaritons.<sup>4</sup> Generated by visible to near-IR light, these surface excitations are tightly confined to the metal/analyte interface. Surface phonon polaritons (SPPs)<sup>5</sup> are supported at the polar crystal/analyte interface and hold great potential for small-volume mid-IR sensing because resonant SPPs, which are sensitive to analyte permittivity ( $\epsilon_a = n_a^2$ ), enhance detection. Studies on SPPs include silicon carbide (SiC),<sup>6,7</sup> AlN,<sup>8</sup> and GaP.<sup>9</sup> Additionally, materials like SiC are durable compared to metal, making them ideal for sensing applications that require contact with hot or chemically aggressive materials.

The main result of this work is that, by exploiting SPP sensitivity to changes in incident angle ( $\theta$ ), vacuum wavelength ( $\lambda$ ), gap spacing ( $d_{\text{gap}}$ ), and the analyte's  $\epsilon_a$ , we show that Otto configuration SPP spectroscopy can enable resonant, small-volume, mid-IR index sensing. The narrow gap required for SPP excitation provides an ideal environment for the study of

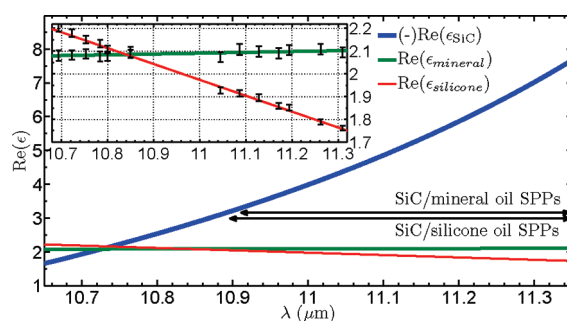


**Figure 1.** Wavelength-dependent permittivities:  $\text{Re}(\epsilon_{\text{SiC}})$ ,  $\text{Re}(\epsilon_{\text{mineral}})$ , and  $\text{Re}(\epsilon_{\text{silicone}})$ . SPPs can be excited when  $\epsilon_{\text{SiC}} < -[\epsilon_{\text{ZnSe}}\epsilon_a/(\epsilon_{\text{ZnSe}} - \epsilon_a)]$ , which corresponds to the ranges indicated above using mineral and silicone oils. Inset: expanded  $\epsilon_{\text{mineral}}$  and  $\epsilon_{\text{silicone}}$ ;  $\Delta\epsilon$  (11.31  $\mu\text{m}$ ) = 0.35, nearly four times greater than  $\Delta\epsilon$  (632.8 nm) = 0.09. Note that  $\epsilon_{\text{silicone}}$  is strongly wavelength-dependent in the mid-IR.

fluid analytes, and the focused laser confines light to a small region, enabling index sensing of volumes as small as 100 pL with resolution down to  $1.5 \times 10^{-3}$  refractive index units<sup>10</sup> (RIU). Sensing was experimentally implemented by performing a reflectivity ( $R$ ) double-scan of  $\theta$  and  $\lambda$  for three analytes—air, mineral oil, and silicone oil—between the surface of SiC and the coupling prism.

Resonant SPP excitation results in electric field enhancement in the gap,<sup>11</sup> thereby enabling enhanced mid-IR sensing and making the detection of weak vibrational bonds possible.<sup>1</sup> Negative  $\epsilon$  in polar crystals results from phonon-polaritons (lattice vibrations). SPPs are supported at the SiC/analyte interface when  $\epsilon_{\text{SiC}} < 0$ ,  $\epsilon_a > 0$ , and  $|\epsilon_{\text{SiC}}| > |\epsilon_a|$ . The SPP dispersion relation for this semi-infinite interface is given by  $k_{\text{SPP}} = \omega/c[\epsilon_{\text{SiC}}\epsilon_a/(\epsilon_{\text{SiC}} + \epsilon_a)]^{1/2}$ .<sup>4</sup> One cannot directly couple radiation to SPPs because the above formula for the propagation wavenumber stipulates that  $k_{\text{SPP}} > \omega/c$ , where  $\omega \equiv 2\pi c/\lambda$ . Therefore, coupling devices such as gratings or prisms are necessary. When a prism is used, either Otto<sup>12</sup> or Kretschmann<sup>4</sup> configuration is employed. This work uses Otto configuration (schematic shown in Figure 3 inset) to excite SPPs, and their presence is detected by attenuated total reflectance (ATR) of  $p$ -polarized (TM) radiation. The prism light line is given by  $k_x = \omega/c[\epsilon_{\text{ZnSe}}]^{1/2} \sin \theta$ , and strong evanescent coupling to SPPs through the hemispherical prism occurs when  $k_x \approx \text{Re}(k_{\text{SPP}})$ .

<sup>†</sup> Part of the "Martin Moskovich Festschrift".

\* Corresponding author. E-mail: gena@physics.utexas.edu.

<sup>‡</sup> University of Texas at Austin.

<sup>§</sup> Université Claude Bernard Lyon 1.

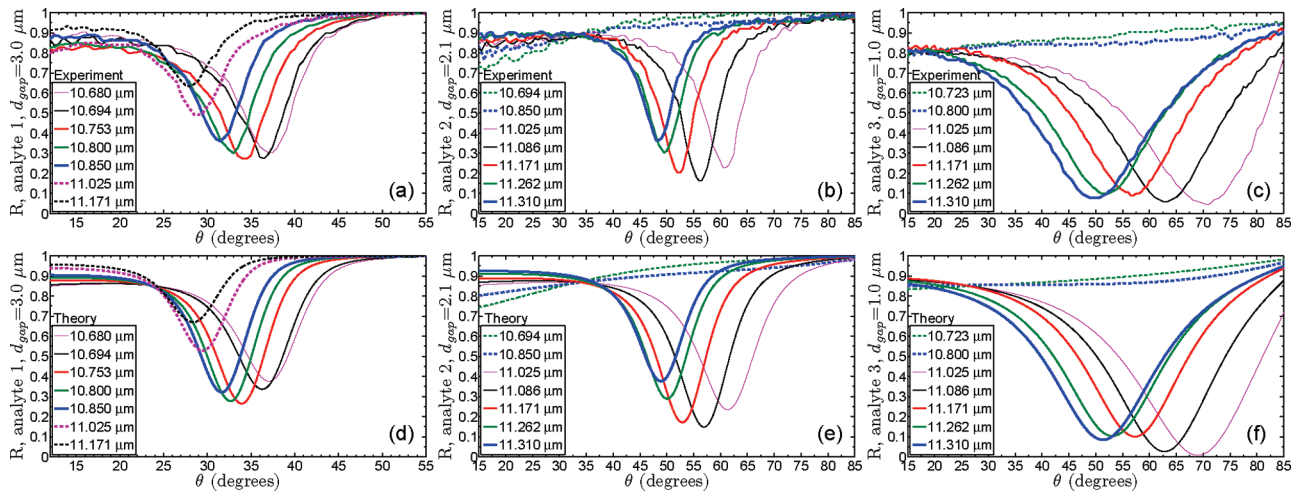


**Figure 2.** Top panel: Experimental plots of reflectivity  $R$  vs  $\theta$  measured in Otto configuration are shown for multiple  $\lambda$ . Bottom panel: corresponding theoretical plots, averaged over an angular spread to match experimental conditions. Left column: a  $3.0\ \mu\text{m}$  layer of analyte 1 (air) is contained between the prism and SiC. Center column:  $2.1\ \mu\text{m}$  layer of analyte 2 (mineral oil). Right column:  $1.0\ \mu\text{m}$  layer of analyte 3 (silicone oil).

Therefore, SiC/analyte SPPs can be excited when  $\epsilon_{\text{SiC}} < -[\epsilon_{\text{ZnSe}}\epsilon_a/(\epsilon_{\text{ZnSe}} - \epsilon_a)]$ , or when  $\text{Re}(\epsilon_{\text{SiC}}) < -3.28$  ( $\lambda > 10.908\ \mu\text{m}$ ) with mineral oil and  $\text{Re}(\epsilon_{\text{SiC}}) < -3.18$  ( $\lambda > 10.894\ \mu\text{m}$ ) with silicone oil, as indicated in Figure 1.

The permittivities of the ZnSe prism, SiC film, and analyte are given by  $\epsilon_{\text{ZnSe}}$ ,  $\epsilon_{\text{SiC}}$ , and  $\epsilon_a$ . Here,  $\epsilon_{\text{SiC}}$  is represented by the polaritonic equation:

$$\epsilon_{\text{SiC}}(\omega) = \epsilon_{\infty} \frac{\omega^2 - \omega_{\text{LO}}^2 + i\gamma\omega}{\omega^2 - \omega_{\text{TO}}^2 + i\gamma\omega} \quad (1)$$

where the longitudinal optical phonon frequency  $\omega_{\text{LO}} = 972\ \text{cm}^{-1}$ , the transverse optical phonon frequency  $\omega_{\text{TO}} = 796\ \text{cm}^{-1}$ , SiC damping  $\gamma = 3.75\ \text{cm}^{-1}$ , and infinite-frequency permittivity  $\epsilon_{\infty} = 6.5$ . These parameters were fit to experimental measurements of transmission through and reflection from an air-bridged SiC membrane.<sup>7</sup> Reflectance calculations shown in Figure 2 required the use of known  $\epsilon_a$ , but neither oil has clear, published data known to the authors. Therefore, total internal reflection (TIR) experiments were performed to characterize  $\epsilon_{\text{oil}} = \epsilon_r + i\epsilon_i$  for large oil depths ( $2.5\ \text{mm}$ ). Reflection is collected as the prism is rotated through the TIR critical angle.  $\epsilon_r$  (plotted in Figure 1) determines  $\theta_{\text{crit}}$  and  $\epsilon_i$  determines the slope of the transition. Wavelength-dependent  $\epsilon_{\text{mineral}}$  and  $\epsilon_{\text{silicone}}$  are represented by polynomial equations that best fit results, with  $\lambda$  ( $\mu\text{m}$ ) in the laser's range given below:  $\epsilon_{\text{mineral}} = 0.0357\lambda + 1.6989 + (-0.0018\lambda + 0.0324)i$ , and  $\epsilon_{\text{silicone}} = -0.6984\lambda + 9.6559 + (0.60994\lambda^3 - 19.6197\lambda^2 + 210.3616\lambda - 751.7636)i$ .

The  $1.5\ \mu\text{m}$  3C-SiC film was grown on Si(100).<sup>11</sup> Infrared radiation was provided by a line-tunable cw  $^{13}\text{CO}_2$  laser, with ranges of  $10.666\text{--}10.867\ \mu\text{m}$  (R branch) and  $11.025\text{--}11.310\ \mu\text{m}$  (P branch). Radiation was focused and then coupled through a  $2.5\ \text{cm}$  ZnSe prism aligned in close proximity to SiC to allow for finite analyte gaps. The schematic, shown in Figure 3, exaggerates the  $2\ \mu\text{m}$  prism face bow ( $40\ \text{m}$  radius of curvature). A HeNe laser ( $632.8\ \text{nm}$ ) was used for in situ gap determination to  $50\ \text{nm}$  accuracy via Fabry–Perot interferometry. For analyte sensing experiments, the gaps were  $d_1 = 3.0\ \mu\text{m}$  for analyte 1 (air),  $d_2 = 2.1\ \mu\text{m}$  for analyte 2 (mineral oil), and  $d_3 = 1.0\ \mu\text{m}$  for analyte 3 (silicone oil). Considering the  $300\ \mu\text{m}$  laser spot size in vacuum, radiation incident through the  $n_{\text{ZnSe}} = 2.4$  index prism, and oblique incidence, we calculate a typical interaction

volume of  $100\ \text{pL}$  using, e.g., a  $2\ \mu\text{m}$  gap. In comparison, an interaction volume of  $\sim 100\ \text{nL}$  was used for SPP-based mid-IR gas index sensing.<sup>3</sup> Numerical results are averaged using a Gaussian angular profile ( $2^\circ$  fwhm) of the incident beam that matches the experimental apparatus. Incident and reflected radiation were measured using a laser power meter. A rotation stage provided angular steps of  $0.5^\circ$ .

In the first sensing experiment, analyte 1 (air) was used with a gap of  $d_1 = 3.0\ \mu\text{m}$ , providing a baseline for fluid sensing because air is a simple dielectric ( $\epsilon_a = 1$ ). In the second sensing experiment, analyte 2 (mineral oil) was used with a gap of  $d_2 = 2.1\ \mu\text{m}$ , and in the third, analyte 3 (silicone oil) was used with a gap of  $d_3 = 1.0\ \mu\text{m}$ . Experimental results, given in Figure 2a–c, show that  $\lambda$ - and  $\theta$ -dependent  $R$  is reproducible by theory, given in Figure 2d–f. All scans display minima and thus finite SPP excitation, but by scanning  $\lambda$ , it is shown that the structure can achieve minimal  $R$  and maximal SPP excitation.<sup>11</sup> Experiments would benefit from a fixed-gap apparatus and therefore a direct analyte sensing comparison. This important technical improvement was outside the scope of this work, but variable-gap prism coupling has been demonstrated.<sup>13</sup> Nevertheless, SPPs were observed for each fluid and gap, demonstrating resonant analyte sensing. Note that for some of the  $R$ -branch laser lines, no excitation of SPPs is observed at the SiC/oil interface because  $\text{Re}(\epsilon) > -3$  for those wavelengths.

In general, index sensing can be implemented using intensity ( $I$ ), angular ( $\theta$ ), or wavelength ( $\lambda$ ) interrogation.<sup>10</sup> System sensitivity  $S_x$ <sup>10</sup> and refractive index resolution  $\delta n_x$ <sup>3</sup> are given by

$$S_x = \frac{dx}{dn_a} \quad \text{and} \quad \delta n_x = \frac{\delta x}{S_x} \quad (2)$$

where  $x$  refers to the interrogation method ( $I$ ,  $\theta$ , or  $\lambda$ ),  $S_x$  is the derivative of the monitored parameter with respect to analyte index, and  $\delta x$  is the minimum parameter change that can be resolved by the sensing system. To demonstrate the sensitivity and resolution of our sensing scheme, we build upon experimental results and propose an apparatus consisting of a fixed-gap SiC channel, a mid-IR source, and a variable- $\theta$  stage that can be tuned to achieve minimal  $R$  and mid-IR index sensing through SPP excitation. We focus on intensity and angular

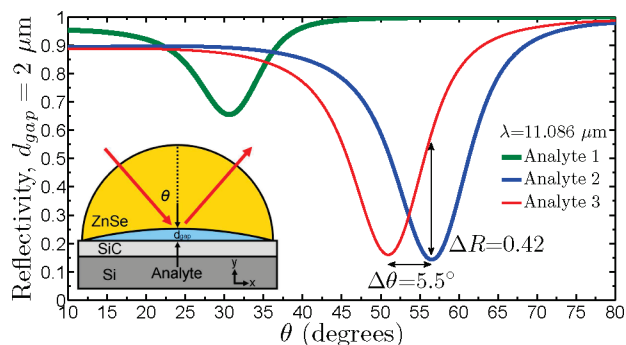


**Figure 3.** Theoretical reflectivity with 2  $\mu\text{m}$  of analytes 1 (air), 2 (mineral oil), and 3 (silicone oil) contained within the gap. Inset: schematic of SPP sensing at the SiC/analyte interface.

interrogation, though wavelength interrogation, which yields resolutions comparable to angular measurements,<sup>10</sup> has been demonstrated in the mid-IR using FTIR spectroscopy.<sup>3</sup> Using  $d_{\text{gap}} = 2 \mu\text{m}$  (which leads to an interaction volume of 100 pL) and  $\lambda = 11.086 \mu\text{m}$ , we calculate reflectivities of 99%, 14%, and 56% for analytes 1, 2, and 3 at  $\theta = 56.5^\circ$ , shown in Figure 3. Here,  $\Delta n_{2,3} = n_2 - n_3 = 0.064 \text{ RIU}$ , or only 4.4% of  $n_2$ , but  $R$  increases by 42%, a 4-fold increase in intensity. This corresponds to a sensitivity of  $S_I = 656\% \text{ RIU}^{-1}$  and a resolution of  $\delta n_I = 1.5 \times 10^{-3} \text{ RIU}$ , where  $\delta I = 1\%$ , limited by the optical system stability, is assumed.

With angular interrogation, the SPP minimum shifts by  $\Delta\theta = 5.5^\circ$  with  $\Delta n_{2,3} = 0.064 \text{ RIU}$  for  $S_\theta = 85.9^\circ \text{ RIU}^{-1}$  sensitivity and  $\delta n_\theta = 5.8 \times 10^{-3} \text{ RIU}$  resolution, where  $\delta\theta = 0.5^\circ$ , corresponding to the minimum angular resolution of the reflection minimum, is assumed. For the present configuration,  $\delta\theta$  is determined by the combination of the beam's profile and prism's geometry. This sensitivity is comparable to  $S_\theta = 78.4^\circ \text{ RIU}^{-1}$  found with a 2D nanohole array SPR sensor at near-IR wavelengths.<sup>14</sup> Near-IR and visible-range experiments offer superior source stabilization and detector sensitivity, leading to resolutions of  $O(10^{-5}) \text{ RIU}$  or better<sup>10,14</sup> when interacting with analyte volumes as small as  $O(1) \text{ nL}$ .<sup>14</sup> Depending on the specific application, it is possible (as we have shown) to interrogate smaller volumes at the expense of resolution.<sup>14</sup> The unique combination of analyte index specificity and pL-volume

sensitivity makes mid-IR SPP excitation a competitive platform for small-volume analyte index sensing.

In conclusion, we have presented small-volume index sensing with analyte specificity based on mid-IR surface phonon-polaritons (SPPs) at the SiC/analyte interface in the Otto configuration, demonstrated by a double-scan of  $\lambda$  and  $\theta$  for three analytes. SPP-based index sensing of pL-scale volumes exploits the SPP resonance conditions and sensitivity to surrounding dielectric properties. Advanced sensing applications are envisioned, with potential to tailor sensing to band-specific applications using SPP-supporting materials such as AlN ( $11.2\text{--}16.4 \mu\text{m}^8$ ) and GaP ( $24.8\text{--}27.4 \mu\text{m}^9$ ).

**Acknowledgment.** The authors thank Dr. Yoav Avitzour for helpful discussions. This work was supported by the National Science Foundation (NSF) NIRT Grant 0709323 and the U.S. Air Force Office of Scientific Research (AFOSR) MURI Grants FA9550-06-1-0279 and FA9550-08-1-0394.

## References and Notes

- (1) Williams, S. M.; Rodriguez, K. R.; Teeters-Kennedy, S.; Shah, S.; Rogers, T. M.; Stafford, A. D.; Coe, J. V. *Nanotechnology* **2004**, *15*, S495.
- (2) Herminjard, S.; Sirigu, L.; Herzig, H.-P.; Studemann, E.; Crottini, A.; Pellaux, J.-P.; Gresch, T.; Fischer, M.; Faist, J. *Opt. Exp.* **2009**, *17*, 293.
- (3) Balin, I.; Dahan, N.; Kleiner, V.; Hasman, E. *Appl. Phys. Lett.* **2009**, *94*, 111112.
- (4) Raether, H. *Surface Plasmons*; Springer-Verlag: New York, 1988.
- (5) Bryksin, V. V.; Gerbshtein, Y. M.; Mirlin, D. N. *Phys. Status Solidi B* **1972**, *51*, 901.
- (6) Huber, A.; Ocelic, N.; Kazantsev, D.; Hillenbrand, R. *Appl. Phys. Lett.* **2005**, *87*, 081103.
- (7) Urzhumov, Y. A.; Korobkin, D.; Neuner III, B.; Zorman, C.; Shvets, G. *J. Opt. A: Pure Appl. Opt.* **2007**, *9*, S322.
- (8) Ng, S. S.; Hassan, Z.; Hassan, H. A. *Appl. Phys. Lett.* **2007**, *90*, 081902.
- (9) Watanabe, J.; Uchinokura, K.; Sekine, T. *Phys. Rev. B* **1989**, *40*, 7860.
- (10) Homola, J.; Yee, S.; Gauglitz, G. *Sens. Actuators B* **1999**, *54*, 3.
- (11) Neuner III, B.; Korobkin, D.; Fietz, C.; Shvets, G.; Carole, D.; Ferro, G. *Opt. Lett.* **2009**, *34*, 2667.
- (12) Otto, A. *Z. Phys.* **1968**, *216*, 398.
- (13) Dawson, P.; Cairns, G. F.; O'Prey, S. M. *Rev. Sci. Instrum.* **2000**, *71*, 4208.
- (14) Tetz, K. A.; Pang, L.; Fainman, Y. *Opt. Lett.* **2006**, *31*, 1528.

JP9114139